

Scale dependence of open $c\bar{c}$ and $b\bar{b}$ production in the low x region

E.G. de Oliveira^{a,b}, A.D. Martin^b and M.G. Ryskin^{b,c}

^a *Departamento de Física, CFM, Universidade Federal de Santa Catarina, C.P. 476, CEP 88.040-900, Florianópolis, SC, Brazil*

^b *Institute for Particle Physics Phenomenology, University of Durham, Durham, DH1 3LE*

^c *Petersburg Nuclear Physics Institute, NRC Kurchatov Institute, Gatchina, St. Petersburg, 188300, Russia*

Abstract

The ‘optimal’ factorization scale μ_0 is calculated for open heavy quark production. We find that the optimal value is $\mu_F = \mu_0 \simeq 0.85\sqrt{p_T^2 + m_Q^2}$; a choice which allows us to resum the double-logarithmic, $(\alpha_s \ln \mu_F^2 \ln(1/x))^n$ corrections (enhanced at LHC energies by large values of $\ln(1/x)$) and to move them into the incoming parton distributions, $\text{PDF}(x, \mu_0^2)$. Besides this result for the single inclusive cross section (corresponding to an observed heavy quark of transverse momentum p_T), we also determined the scale for processes where the acoplanarity can be measured; that is, events where the azimuthal angle between the quark and the antiquark may be determined experimentally. Moreover, we discuss the important role played by the $2 \rightarrow 2$ subprocesses, $gg \rightarrow Q\bar{Q}$ at NLO and higher orders. In summary, we achieve a better stability of the QCD calculations, so that the data on $c\bar{c}$ and $b\bar{b}$ production can be used to further constrain the gluons in the small x , relatively low scale, domain, where the uncertainties of the global analyses are large at present.

1 Introduction

The present global PDF analyses (e.g. NNPDF3.0 [1], MMHT2014 [2], CT14 [3]) find that there is a large uncertainty in the low x behaviour of the gluon distribution. There is a lack of appropriate very low x data, particularly at low scales. However, recently measurements on

open charm and open beauty in the forward direction have been presented by the LHCb collaboration [4, 5, 6, 7]; moreover, the ATLAS collaboration has measured open charm production in the central rapidity region [8]. These data sample the gluon distribution at rather low x : namely in the domain $10^{-5} \lesssim x \lesssim 10^{-4}$. A discussion of the data in terms of existing global PDFs has been presented in [9, 10], and they have been incorporated in a fit with the HERA deep inelastic data in [11].

In the ideal case it would be good to have such data where both the heavy quark and the heavy antiquark were measured, since when we observe only one quark (one heavy hadron) the value of x that is probed is smeared out over an order of magnitude by the unknown momentum of the unobserved quark in the $Q\bar{Q}$ -pair [12, 9], where $Q \equiv c, b$, see e.g. Fig.1 in [9]. Nevertheless, even measurements of the inclusive cross section of one heavy quark can be used to check and further constrain the existing PDFs.

Another problem, which was emphasized in [10], is that the QCD prediction at NLO level strongly depends on the factorization scale, μ_F , assumed in the calculation. We might expect that the major source of the strong μ_F dependence arises because in the DGLAP evolution of low x PDFs the probability of emitting a new gluon is strongly enhanced by the large value of $\ln(1/x)$. Indeed, the mean number of gluons in the interval $\Delta \ln \mu_F^2$ is [13]

$$\langle n \rangle \simeq \frac{\alpha_s N_C}{\pi} \ln(1/x) \Delta \ln \mu_F^2, \quad (1)$$

leading to a value of $\langle n \rangle$ up to about 8, for the case $\ln(1/x) \sim 8$ with the usual μ_F scale variation interval from $\mu_F/2$ to $2\mu_F$. In contrast, the NLO coefficient function allows for the emission of only *one* gluon. Therefore we cannot expect compensation between the contributions coming from the PDF and the coefficient function as we vary the scale μ_F . It was shown in [14, 15] that this strong double-logarithmic part of the scale dependence can be successfully resummed by choosing an appropriate scale, μ_0 , in the PDF convoluted with the LO hard matrix element, which in our case is $\mathcal{M}(gg \rightarrow Q\bar{Q})$.

The outline of the paper is as follows. In Section 2 we recall the method of performing the resummation to determine the optimal scale μ_0 . In Section 3 we justify choosing the renormalization scale equal to the factorization scale. Then in Section 4.1 we use the procedure discussed in Section 2, to resum the $\ln(1/x)$ terms so as to determine the optimum factorization scale, μ_0 . Unfortunately for heavy $Q\bar{Q}$ production (unlike the Drell-Yan process) a large sensitivity to the choice of scale remains. In Section 4.2 we identify the source of the problem to be the important $2 \rightarrow 2$ (that is $gg \rightarrow Q\bar{Q}$) diagrams at NLO and higher orders. We argue that it is possible to also resum these diagrams. We then find the scale sensitivity is reduced. It would be advantageous if both heavy mesons (arising from Q and \bar{Q}) could be measured experimentally, but, at present, the statistics are limited. However, a possibility to circumvent this problem is discussed in Section 5. In Section 6 we return to open single inclusive $c\bar{c}$ and $b\bar{b}$ production and compare the QCD predictions with the optimal scale with LHC data; and are able to make an observation about the gluon PDF at low x . In Section 7 we present our conclusion.

2 Way to choose the optimum factorization scale

Here we recall the procedure proposed in [14, 15], which provides a reduction in the sensitivity to the choice of factorization scale by resumming the enhanced double-logarithmic contributions from a knowledge of the NLO contribution. The cross section for open heavy quark production at LO + NLO at factorization scale μ_f may be expressed in the form¹

$$\sigma^{(0)}(\mu_f) + \sigma^{(1)}(\mu_f) = \alpha_s^2 [\text{PDF}(\mu_f) \otimes C^{(0)} \otimes \text{PDF}(\mu_f) + \text{PDF}(\mu_f) \otimes \alpha_s C^{(1)}(\mu_f) \otimes \text{PDF}(\mu_f)] , \quad (2)$$

where the coefficient function $C^{(0)}$ does not depend on the factorisation scale, while the μ_f dependence of the NLO coefficient function arises since we have to subtract from the NLO diagrams the part already generated by LO evolution.

We are free to evaluate the LO contribution at a different scale μ_F , since the resulting effect can be *compensated* by changes in the NLO coefficient function, which then also becomes dependent on μ_F . In this way eq. (2) becomes

$$\sigma^{(0)}(\mu_f) + \sigma^{(1)}(\mu_f) = \alpha_s^2 [\text{PDF}(\mu_F) \otimes C^{(0)} \otimes \text{PDF}(\mu_F) + \text{PDF}(\mu_f) \otimes \alpha_s C_{\text{rem}}^{(1)}(\mu_F) \otimes \text{PDF}(\mu_f)] . \quad (3)$$

Note that although the first and second terms on the right hand side depend on μ_F , their sum, however, does not (to $\mathcal{O}(\alpha_s^4)$), and is equal to the full LO+NLO cross section calculated at the factorization scale μ_f .

Originally the NLO coefficient functions $C^{(1)}$ are calculated from Feynman diagrams which are independent of the factorization scale. How does the μ_F dependence of $C_{\text{rem}}^{(1)}$ in (3) actually arise? It occurs because we must subtract from $C^{(1)}$ the α_s term which was already included in the LO contribution. Since the LO contribution was calculated up to some scale μ_F the value of $C^{(1)}$ after the subtraction depends on the value μ_F chosen for the LO component. The change of scale of the LO contribution from μ_f to μ_F also means we have had to change the factorisation scale which enters the coefficient function $C^{(1)}$ from μ_f to μ_F . The effect of this scale change is driven by the LO DGLAP evolution, which is given by

$$\sigma^{(0)}(\mu_F) = \alpha_s^2 \text{PDF}(\mu_f) \otimes \left(C^{(0)} + \frac{\alpha_s}{2\pi} \ln \left(\frac{\mu_F^2}{\mu_f^2} \right) (P_{\text{left}} \otimes C^{(0)} + C^{(0)} \otimes P_{\text{right}}) \right) \otimes \text{PDF}(\mu_f) , \quad (4)$$

where P_{left} and P_{right} denote DGLAP splitting functions acting on the PDFs to the left and right respectively. That is, by choosing to evaluate $\sigma^{(0)}$ at scale μ_F we have moved the part of the NLO (i.e. α_s) corrections given by the last term of (4) from the NLO to the LO part of the cross section. In this way $C^{(1)}$ becomes the remaining μ_F -dependent coefficient function $C_{\text{rem}}^{(1)}(\mu_F)$ of (3). The idea is to choose a scale $\mu_F = \mu_0$ such that the remaining NLO term does not contain the double-logarithmic $(\alpha_s \ln(\mu_F) \ln(1/x))^n$ contributions. It is impossible to

¹For ease of understanding we omit the parton labels $a = g, q$ on the quantities in (2) and the following equations. The matrix form of the equations is implied.

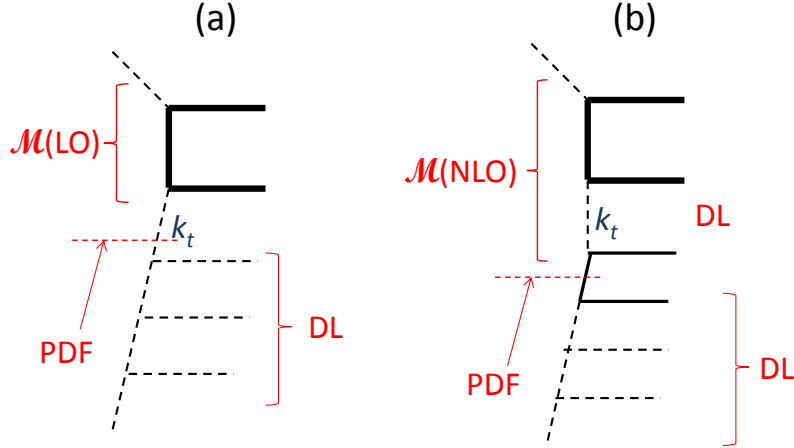


Figure 1: Heavy quark production at (a) LO via the $gg \rightarrow Q\bar{Q}$ subprocess, and (b) via the $qq \rightarrow Q\bar{Q}q$ subprocess. The diagrams with s -channel gluons ($g^* \rightarrow Q\bar{Q}$) are not shown for simplicity. Moreover, only the PDF below the hard matrix element, \mathcal{M} , is shown. Note that the double logarithmic (DL) integral in the NLO matrix element is exactly the same as in the first gluon cell below the LO matrix element. In both cases the ultraviolet convergence is provided by the k_t dependence of the respective matrix element. Therefore it is possible to move the large DL contribution from the coefficient function $C^{(1)}$ of the NLO term, diagram (b), to the PDF term in the LO diagram (a) by choosing an appropriate value of μ_F , and in this way to resum all the higher order DL contributions in the PDFs(μ_F) of the LO diagram (a).

nullify the whole NLO contribution since the function $C^{(1)}(\mu)$ depends also on other variables; in particular, it depends on the mass, \hat{s} , of the system produced by the hard matrix element. On the other hand we can choose such a value of μ which makes $C^{(1)}(\mu, \hat{s}) = 0$ in the limit of large $\hat{s} \gg m_Q^2$. Recall that the $\ln(1/x)$ factor arises in the NLO after the convolution of the large \hat{s} asymptotics of hard subprocess cross section with the incoming parton low- x distributions satisfying

$$xq(x) \rightarrow \text{constant} \quad \text{or} \quad xg(x) \rightarrow \text{constant}. \quad (5)$$

At NLO level the change μ_f to μ_F is irrelevant: eq.(3) is an identity (it just changes the higher order terms). However, in this way we simultaneously resum all the higher order double-logarithmic contributions in the PDFs(μ_F) of the LO part. As a result we are able to suppress the scale dependence caused by large values of $\log(1/x)$.

Thus the choice of $\mu = \mu_0$, which nullifies $C^{(1)}$ at large $\hat{s} \gg m_Q^2$, excludes the Double Log (DL), $\alpha_s \ln \mu_F^2 \ln(1/x)$, contribution from the NLO correction by resumming the series of double-logarithmic terms in the PDFs, which are then convoluted with the LO coefficient functions. To find the appropriate value of μ_0 we must choose the NLO subprocess driven by the same ladder-type diagrams (in the axial gauge) as the ladder diagrams that describe

LO DGLAP evolution. The appropriate subprocess is gluon-light quark fusion, $gq \rightarrow Q\bar{Q}q$. In the high energy limit, where the subprocess energy satisfies $\hat{s}(gq) \gg m_Q^2$, the cross section described by this subprocess contains double-logarithmic terms $\log(\mu_F^2/\mu_0^2) \log(\hat{s}/m_Q^2)$. The subprocess $gq \rightarrow Q\bar{Q}q$ is contained in the sketch of Fig. 1(b), where it is shown pictorially how the enhanced double-logarithmic terms are transferred to the PDFs in the LO term.

2.1 Extension to higher orders

We note that, in general, this decomposition can be continued to higher order. For example, if the NNLO contribution is known, then we will have three scales: μ_f , $\mu_F = \mu_0$ and μ_1 ,

$$\begin{aligned} \sigma^{(0)}(\mu_f) + \sigma^{(1)}(\mu_f) + \sigma^{(2)}(\mu_f) = & \alpha_s^2 [\text{PDF}(\mu_0) \otimes C^{(0)} \otimes \text{PDF}(\mu_0) + \\ & \text{PDF}(\mu_1) \otimes \alpha_s C_{\text{rem}}^{(1)}(\mu_0) \otimes \text{PDF}(\mu_1) + \text{PDF}(\mu_f) \otimes \alpha_s^2 C_{\text{rem}}^{(2)}(\mu_0, \mu_1) \otimes \text{PDF}(\mu_f)] , \quad (6) \end{aligned}$$

where the scale μ_1 is chosen to nullify the final term in the small x limit.

In fact in Section 4.2 we will use this equation to include the important $2 \rightarrow 2$ (that is, $gg \rightarrow Q\bar{Q}$) subprocess at NLO and higher orders. We will show reasons why the scale choice $\mu_1 = \mu_0$ will give a good approximation for the resummation of these higher-order $2 \rightarrow 2$ contributions.

2.2 Comparison with k_t factorization

The approach we have introduced is based on collinear factorization. However, actually it is close in spirit to the k_t -factorization method. Indeed, there, the value of the factorization scale is driven by the structure of the integral over k_t , see Fig. 2. In the k_t -factorization approach this k_t integral is written explicitly, while the parton distribution *unintegrated* over k_t is generated by the last step of the DGLAP evolution, similar to the prescription proposed in Refs. [16, 17]. Then, using the known NLO result, we account for the *exact* k_t integration in the last cell adjacent to the LO hard matrix element. This hard matrix element \mathcal{M} , provides the convergence of the integral at large k_t . In this way it puts an effective upper limit of the k_t integral, which plays the role of an appropriate factorization scale.

3 The renormalization scale μ_R

Besides the factorization scale, the QCD prediction, truncated at NLO, strongly depends on the renormalization scale μ_R , since the LO term is already proportional to $\alpha_s^2(\mu_R)$. Let us discuss the possible choice of μ_R . First, it is reasonable to have $\mu_R \gtrsim \mu_F$, since we expect all the contributions with virtualities less than μ_F to be included in the PDFs, while those larger than μ_F to be assigned to the hard matrix element. This is in line with the fact that the

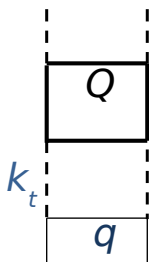


Figure 2: The diagram for AA^* , where A is the amplitude for the subprocess $gg \rightarrow Q\bar{Q}q$ shown in Fig. 1(b). However, in the k_t factorization approach k_t is integrated over and the effective upper limit of the convergent integral essentially plays the role of the appropriate factorization scale.

current scale of the QCD coupling increases monotonically during the DGLAP evolution. So the coupling responsible for heavy quark production should have a scale μ_R equal to, or larger than, that in the evolution.

Another argument is based on the BLM prescription [18], which says that all the contributions proportional to $\beta_0 = 11 - \frac{2}{3}n_f$ should be assigned to α_s by choosing an appropriate scale μ_R . A good way to trace the β_0 contribution is to calculate the LO term generated by a new type of light quark, so $n_f \rightarrow n_f + 1$. Note that the new quark-loop insertion appears twice in the calculation. The part with scales $\mu < \mu_F$ is generated by the virtual ($\propto \delta(1-z)$) component of the LO splitting during DGLAP evolution, while the part with $\mu > \mu_R$ accounts for the running α_s behaviour obtained after the regularization of the ultraviolet divergence. In order not to miss some contribution and to avoid double counting we take the renormalization scale $\mu_R = \mu_F$. The argument for this choice was made in more detail in [19] for the QED case.

We emphasize (see also [10]) that the renormalisation scale dependence affects just the normalization of cross section, but not its energy behaviour. It is cancelled in the ratio of the cross sections measured at the LHC energy of 7 (or 8 or 5) TeV to that at 13 TeV or in the ratio of the cross sections obtained at different rapidities. Thus these ratios will probe the low x dependence of the gluons at scale $\mu_F = \mu_0$ essentially without any uncertainties due to possible variations of the μ_R scale.

4 Sensitivity of predictions to the factorization scale

Here we implement the proposals of eqs. (3) and (6) in an attempt to reduce the factorization scale dependence of the QCD predictions for $Q\bar{Q}$ production in high-energy $p\bar{p}$ collisions. Note, however, that calculating the NLO contribution of the diagram in Fig. 1, we have integrated over the momenta of other particles; in particular, over the transverse momentum, $-k_t$, of the light quark.

4.1 The optimum scale to resum $\ln(1/x)$ terms

We use the formulae from appendix B of the [20] paper to calculate the $gg \rightarrow Q\bar{Q}q$ matrix element in the high energy limit in order to find a scale,

$$\mu_F \equiv \mu_0 = F * \sqrt{p_T^2 + m_Q^2}, \quad (7)$$

that nullifies the double-logarithmic NLO contribution: that is, to find a scale μ_0 at which the DGLAP-induced contribution ($P_{\text{left}} \otimes C^{(0)} + C^{(0)} \otimes P_{\text{right}}$) replaces the NLO correction calculated explicitly. Note, however, that calculating the NLO contribution of the diagram in Fig. 1, we have integrated over the momenta of other particles; in particular, over the transverse momentum, $-k_t$, of the light quark. Since we are going to consider the upper (heavy quark) box in Fig. 1 as the ‘hard’ subprocess, and would like to keep the DGLAP k_t ordering, we put an additional cut $-|k_t| < \min\{m_{TQ}, m_{T\bar{Q}}\}$; otherwise the lower part of diagram (which may be either qQ or $q\bar{Q}$ scattering) may have $k_t > m_T$, and would then be treated as the hard subprocess. Here $m_T = \sqrt{m_Q^2 + p_T^2}$.

The values that we find for the ‘optimal’ scale μ_0 are presented in Fig. 3 as the function of p_T/m_Q ratio, where p_T is the transverse momentum of the observed heavy quark. It turns out that the values of the optimal scale are close to the value $\mu_F^2 = m_T^2 \equiv p_T^2 + m_Q^2$ that is used conventionally; that is $F = 1$. However, we now have a physics justification for the scale choice shown in Fig. 3, which to a good approximation is $\mu_0 \simeq 0.85m_T$, that is $F \simeq 0.85$.

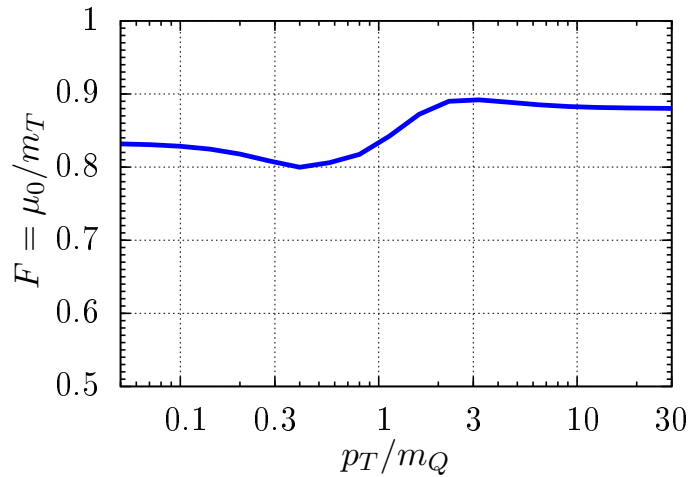


Figure 3: The optimal scale, $\mu_0 = Fm_T$, as a function of p_T/m_Q .

Now that we have the value of μ_0 , we can study the factorization scale, μ_f , dependence of the QCD predictions for $c\bar{c}$ and $b\bar{b}$ production. The results are shown in Fig. 4 for a Q quark of pseudorapidity $\eta = 3$ – typical of the LHCb experiment. We use the CT14 [3] PDFs as an example of a recent set of partons which have no negative gluon distributions and take the

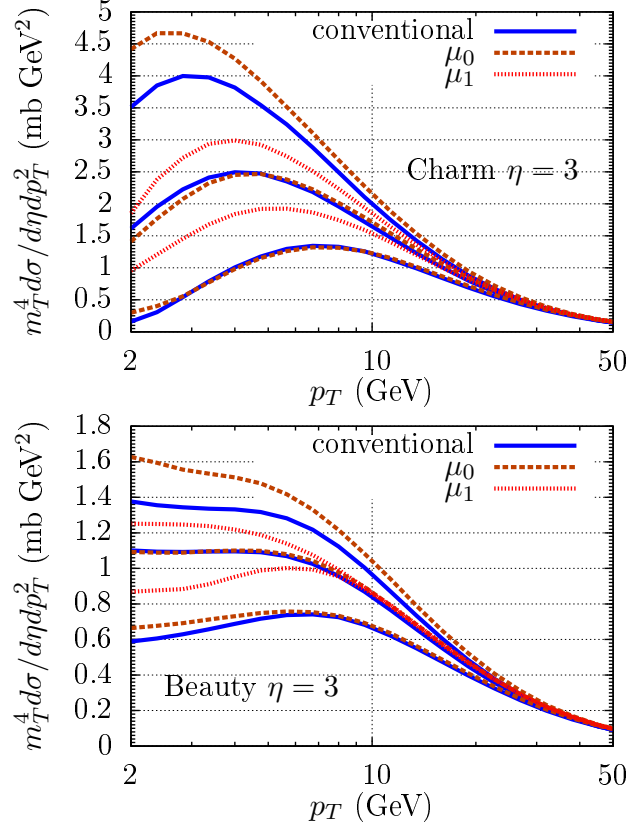


Figure 4: The scale dependence of the predictions of the cross section, $m_T^4 d\sigma/d\eta dp_T^2$, for $c\bar{c}$ and $b\bar{b}$ production respectively, using the NLO CT14 parton set. The plot shows the scale variation $\mu_f = (2, 1, 0.5)m_T$ for three different procedures: (i) the conventional prediction (blue curves), (ii) resumming the $\ln(1/x)$ contributions with $\mu_F = \mu_0 \simeq 0.85m_T$ in (3) (dashed red curves), (iii) in addition resumming the $2 \rightarrow 2$ contributions with $\mu_1 = \mu_0$ in (6) (dotted red curves).

corresponding heavy quark masses: $m_c = 1.3$ GeV and $m_b = 4.75$ GeV. Subroutines from the MCFM [21] and FONLL [22] programmes were used for the computations.

For simplicity we take $F = 0.85$, that is, $\mu_0 = 0.85m_T$, and make predictions for three different values of the factorization scale μ_f , namely $\mu_f = (0.5, 1, 2)m_T$. The results are shown in Fig. 4 by the dashed red curves. We repeat the cross section prediction, but now use (2) with the conventional choice $\mu_f = (0.5, 1, 2)m_T$, which gives the blue curves. Not surprisingly, since the optimum scale is close to the conventional choice $\mu_0 = m_T$, the scale uncertainties are comparable.

Unfortunately we still have rather strong dependence of the predicted cross section on the choice of the value of μ_f . It is caused by the relatively low mass contribution coming mainly from the $2 \rightarrow 2$ ($gg \rightarrow Q\bar{Q}$) component of $C^{(1)}$. This component does not contain a $\ln(1/x)$ dependence, but, at our low scales, it is numerically large; it gives up to twice as large a contribution as the LO one. Moreover, being convoluted with low- x PDFs, which strongly

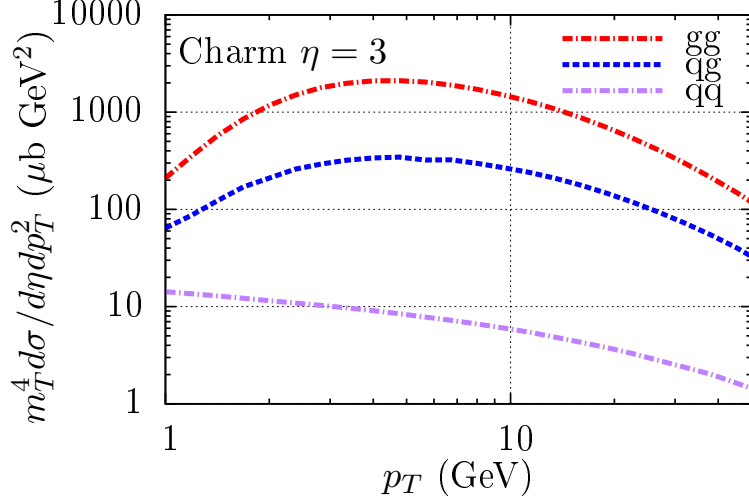


Figure 5: The gg , qg , $q\bar{q}$ fusion contributions to $c\bar{c}$ production for a charm quark produced at pseudorapidity $\eta = 3$ at in pp collisions at 13 TeV

depend on μ_f , it produces a large scale uncertainty.

4.2 The optimum scale to resum the higher-order $2 \rightarrow 2$ diagrams

The important $2 \rightarrow 2$ NLO contributions are mainly the NLO-loop corrections to the *renormalization* scale used in the LO part, together with ‘soft’ corrections of Sudakov origin. This was demonstrated for the case of $t\bar{t}$ production, for example in Fig. 6 of [23]. It means that they are similar kinematically to the LO contributions to the cross section. That is, the upper limit (cut) in the DGLAP evolution convoluted with these diagrams should be just the ‘same’ as in the LO case. Thus it looks reasonable to convolute these terms with the same PDFs as those used for the LO evaluation. This will provide the correct resummation of the higher-order DL terms, $(\alpha_s \ln \mu_F \ln(1/x))^n$ (with $n = 2, 3, \dots$) inside the incoming parton distributions. Referring to (6), it means that we may argue that the scale $\mu_1 = \mu_0$ for the $2 \rightarrow 2$ part of coefficient function $C^{(1)}$. The corresponding curves, calculated from (6) with $\mu_1 = \mu_0$, are shown in Fig. 4 by the dotted red curves. We see that the remaining μ_f dependence is much reduced. We consider this observation as a strong argument in favour of the possibility to use the open charm/beauty data to constraint the low x partons at the scale $\mu_f = 0.85m_T$.

Since the major contribution to $c\bar{c}$ and $b\bar{b}$ production comes from gluon-gluon fusion (see Fig. 5), including these data in global parton analyses will allow a better study of the gluon low- x behaviour, and hence to strongly diminish the present uncertainty observed in this region.

ϕ_0	0.0875	0.175	0.263	0.350	0.438	0.525	radians
	5°	10	15	20	25	30	degrees
μ_0/m_b	0.17	0.33	0.46	0.58	0.69	0.78	
μ_0	0.83	1.57	2.20	2.76	3.26	3.70	GeV

Table 1: The optimal factorization scale, μ_0 , corresponding to a coplanarity cut $\Delta\phi < \phi_0$ for events with both heavy quarks in the rapidity interval $2 < y < 4.5$. The cross section is integrated over the heavy quark transverse momenta p_T .

5 Azimuthal cut to reduce optimal scale for $b\bar{b}$ events

In the case of open $b\bar{b}$ production the optimal scale is rather large; typically $\mu_0^2 > 30 \text{ GeV}^2$. On the other hand, the main uncertainties in the gluon PDF are observed at much lower scales $\sim 2 - 4 \text{ GeV}^2$. One possibility to reduce the scale at which the process probes the partons is to observe both heavy quarks (i.e. both the quark and the antiquark), and then to select the events where the transverse momentum of the pair is small. This proposal was discussed in [12] (and in [14] for Drell-Yan pair production). Unfortunately, the *transverse momenta* of B mesons can only be measured for a few particular decay modes, and the product of the branching ratios for the two B mesons is small. It means that we do not have sufficient statistics.

Another idea was proposed by Alexey Dzyuba². As a rule the vertex of B meson decay can be observed experimentally, and it is possible to measure the *azimuthal angle*, ϕ , between the two heavy mesons. That is, we may select $B\bar{B}$ events with good coplanarity. In such a case the transverse momenta of the incoming partons must be small, otherwise the coplanarity will be destroyed. In other words, for events with a small $\Delta\phi = \pi - \phi$ we deal with lower scale partons. For example, in Table 1 we show the optimal scale $\mu_0(\Delta\phi)$ calculated for events with $\Delta\phi < \phi_0$ corresponding to the LHCb rapidity interval $2 < y < 4.5$. As expected, for low ϕ_0 we have $\mu_0 \propto \phi_0$. For instance, for $b\bar{b}$ production with $\Delta\phi < 10^\circ$ one can probe gluons at a rather low scale, namely $\mu \simeq 1.5 \text{ GeV}$.

6 Comparison with $c\bar{c}$ and $b\bar{b}$ data

Now that we have the optimal factorization scale, $\mu_0 \simeq 0.85m_T$, we can make an exploratory comparison with the existing LHC data for open single inclusive heavy-flavour production. To compare with the data we use the subroutines from MCFM and FONLL programmes [21, 22]. The QCD description of the present data in the low- x , low- μ domain is shown in Fig. 6. As an example, we consider just the D^+ (B^+) meson cross sections using the probabilities of the quark to meson transition $P(c \rightarrow D^+) = 0.25$ and $P(b \rightarrow B^+) = 0.25$. We account for the fact that the D/B meson momentum is less than that of the parent quark by making the assumption

²We thank Alexey Dzyuba of the Petersburg Nuclear Physics Institute for this idea.

that $p_D \sim 0.75p_c$ and $p_B \sim 0.9p_b$ (see [24, 25]). It is seen that the QCD prediction obtained using the ‘optimal’ factorization scale underestimates the LHCb data. Moreover, for $c\bar{c}$ the cross section in the central region predicted by FONLL is also about twice (1.88) lower than the ATLAS data [8]. The overall comparison indicates that the input low- x gluon PDF³ should be larger than the central values that found in CT14 NLO PDF set. The same conclusion is valid for the PDFs from other global analyses.

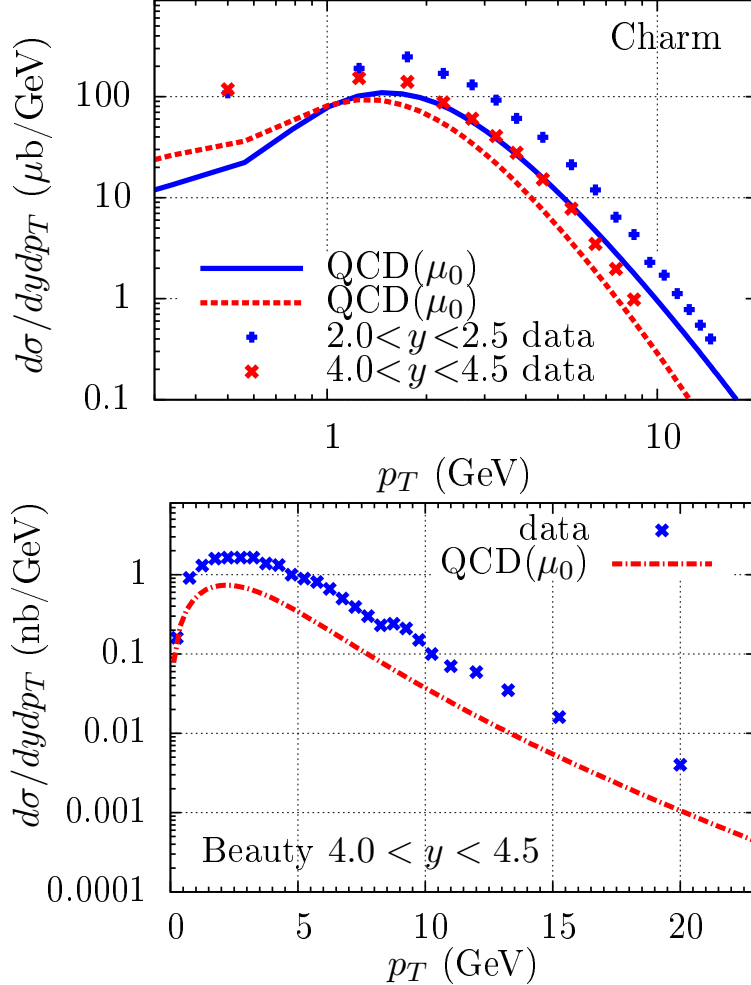


Figure 6: The QCD predictions for the cross section for heavy meson (D^+ , B^+) production compared with LHCb data [5, 7], as a function of the p_T of the heavy meson. In the upper plot the blue (red) curves and data points, taken at $\sqrt{s}=13$ TeV, correspond to the D^+ rapidity bins $2 < y < 2.5$ ($4 < y < 4.5$) respectively; whereas the lower plot corresponds to B^+ rapidity in the interval $4 < y < 4.5$ for a collider energy of $\sqrt{s}=7$ TeV. CT14 NLO PDFs [3] are used. The optimal factorization scale is taken $\mu_F = \mu_0 = \mu_1 = 0.85m_T$; and the renormalization scale is taken to be $\mu_R = \mu_F$, see Section 3.

³Recall that the heavy quark cross section comes mainly from gluon-gluon fusion, see Fig 5. The $q\bar{q}$ and the gg contributions gives about 15% for $c\bar{c}$ production; and even less for $b\bar{b}$ production.

7 Conclusion

We have calculated the ‘optimal’ factorization scale, μ_0 , which allows a resummation of the higher-order α_s corrections, enhanced at high energies by the large $\ln(1/x)$ factor; that is to resum the double logarithmic, $(\alpha_s \ln \mu_F^2 \ln(1/x))^n$, terms and move them into the incoming parton distributions. The result is given in Fig. 3. It is essentially

$$\mu_F = \mu_0 \simeq 0.85 \sqrt{p_T^2 + m_Q^2} \quad (8)$$

for single open inclusive heavy quark production, where p_T is the transverse momentum of the observed heavy quark.

We also considered the case when the azimuthal angle, ϕ , between the heavy quark and the antiquark can be measured. We showed that by selecting events with small $\Delta\phi = \pi - \phi$ we are able to probe smaller factorization scales μ_0 . This is an advantage for $b\bar{b}$ production: compare the results of Table 1 with eq. (8). The disadvantage is that the rate is smaller for such events, even though we do not require that the transverse momentum of both the heavy quarks are measured.

The choice $\mu_F = \mu_0$ reduces the uncertainty of the perturbative QCD calculations. It allows us to argue that the recent LHC data on $c\bar{c}$ and $b\bar{b}$ production show evidence in favour of larger low- x gluon densities than those given by the central values of the present global analyses. In summary, we conclude that $c\bar{c}$ and $b\bar{b}$ data can be used to further constrain the behaviour of the gluon distribution in the region of very small x and low scale, equal to μ_0 , where the uncertainties of the present global parton analyses are especially large.

Acknowledgments

We thank Keith Ellis for valuable discussions. MGR and EGdO thank the IPPP at the University of Durham for hospitality. This work was supported by the RSCF grant 14-22-00281 for MGR and by Capes and CNPq (Brazil) for EGdO.

References

- [1] R.D. Ball *et al.* [NNPDF Collaboration], JHEP **1504** (2015) 040.
- [2] L.A. Harland-Lang, A.D. Martin, P. Motylinski and R.S. Thorne, Eur. Phys. J. **C75** (2015) 5, 204.
- [3] S. Dulat, T.J. Hou, J. Gao, M. Guzzi, J. Huston, P. Nadolsky, J. Pumplin, C. Schmidt, D. Stump and C.P. Yuan, Phys. Rev. **D93** (2016) 033006 [[arXiv:1506.07443](#)].

- [4] R. Aaij *et al.* [LHCb Collaboration], Nucl. Phys. **B871** (2013) 1.
- [5] R. Aaij *et al.* [LHCb Collaboration], JHEP **1603** (2016), 159.
- [6] R. Aaij *et al.* [LHCb Collaboration], arXiv:1610.02230 [hep-ex].
- [7] R. Aaij *et al.* [LHCb Collaboration], JHEP **1308** (2013) 117.
- [8] G. Aad *et al.* (ATLAS collaboration), Nucl.Phys. **B907** (2016) 717 [arXiv: 1512.02913].
- [9] R. Gauld, J. Rojo, L. Rottoli and J. Talbert, JHEP **1511** (2015) 009 [arXiv:1506.08025].
- [10] M. Cacciari, M. L. Mangano and P. Nason, Eur. Phys. J. **C75** (2015) 610.
- [11] O. Zenaiev *et al.*, Eur. Phys. J. **C75** (2015) 396.
- [12] E.G. de Oliveira, A.D. Martin and M.G. Ryskin, Eur. Phys. J. **C71** (2011) 1727.
- [13] Y.L. Dokshitzer, D. Diakonov and S. Troian, Phys. Rept. **58** (1980) 269.
- [14] E.G. de Oliveira, A.D. Martin, M.G. Ryskin, Eur.Phys.J. **C73** (2013) 2361,
Eur. Phys. J. **C72** (2012) 2069.
- [15] S.P. Jones, A.D. Martin, M.G. Ryskin and T. Teubner, J. Phys. **G43** (2016) 035002
[arXiv:1507.06942].
- [16] M.A. Kimber, A.D. Martin and M.G. Ryskin, Phys. Rev. **D63** (2001) 114027.
- [17] A.D. Martin, M.G. Ryskin and G. Watt, Eur. Phys. J. **C66** (2010) 163.
- [18] S.J. Brodsky, G.P. Lepage and P.B. Mackenzie, Phys. Rev. **D28** (1983) 228.
- [19] L.A. Harland-Lang, M.G. Ryskin and V.A. Khoze, Phys. Lett. **B761** (2016) 20
[arXiv:1605.04935].
- [20] S. Catani, M. Ciafaloni, F. Hautmann Nucl.Phys. **B366** (1991) 135.
- [21] P. Nason, S. Dawson and R.K. Ellis, Nucl. Phys. **B327** (1989) 49.
- [22] M. Cacciari, M. Greco and P. Nason, JHEP **9805** (1998) 007.
- [23] C. Muselli, M. Bokvini, S. Forte, S. Marzani and G. Ridolfi, JHEP **1508** (2015) 076.
- [24] Particle Data Group, Chinese Physics **C35** (2014) 090001.
- [25] M. Cacciari, S. Frixione, N. Houdeau, M. L. Mangano, P. Nason and G. Ridolfi, JHEP **1210** (2012) 137 [arXiv:1205.6344].